JACS
JOURNAL OF THE AMERICAN CHEMICAL SOCIETY
pubs.acs.org/JACS
Article

Air-Stable Thermoluminescent Carbodicarbene-Borafluorenium Ions

Kimberly K. Hollister, Andrew Molino, Grace Breiner, Jacob E. Walley, Kelsie E. Wentz, Ashley M. Conley, Diane A. Dickie, David J. D. Wilson,* and Robert J. Gilliard, Jr.*

Cite This: J. Am. Chem. Soc. 2022, 144, 590−598
Read Online

ABSTRACT: Borenium ions, originally synthesized as fundamentally important laboratory curiosities, have attracted significant attention due to their applications in catalysis and frustrated Lewis pair chemistry. However, investigations of the materials properties of these types of compounds are exceptionally rare. Herein, we report the synthesis, molecular structures, and optical properties of a new class of air-stable borenium ions, stabilized by the strongly donating carbodicarbene (CDC) ligand (**2**, **3**, **6**). Notably, CDC-borafluorenium ions exhibit thermoluminescence in solution, a result of a twisted intramolecular charge transfer process. The temperature responsiveness, which is observable by the naked eye, is assessed over a 20 to −60 °C range. Significantly, compound **2** emits white light at lower temperatures. In the solid state, these borocations exhibit increased quantum yields due to aggregation-induced emission. CDC-borafluorenium ions with two different counteranions (Br^-, BPh_4^-) were investigated to evaluate the effect of anion size on the solution and solid-state optical properties. In addition, CDCs containing both symmetrical and unsymmetrical N-heterocycles (bis(1-isopropyl-3-methylbenzimidazol-2-ylidene)methane and bis(1,3-dimethyl-1,3-dihydro-2*H*-benzo[*d*]imidazol-2-ylidene)methane) were tested to understand the implications of free rotation about the CDC ligand carbon−carbon bonds. The experimental work is complemented by a comprehensive theoretical analysis of the excited-state dynamics.

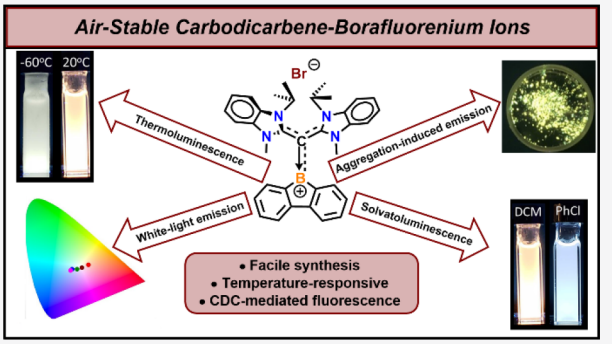

INTRODUCTION

Over three decades ago Nöth and co-workers reported the first examples of borenium ions, introducing a new class of positively charged tricoordinate boron species with the general formula $[LBR_2]^+$ (L = ligand; R = generic functional group).[1] At the time, these borocations were largely regarded as laboratory curiosities, as the highly electrophilic boron center rendered these molecules reactive and synthetically challenging to isolate.[2] In the intervening years, borenium ions have become powerful reagents in chemical synthesis and catalysis.[2,3] Despite the near 40-year gap since the original report of Nöth's acridine-borafluorenium ion (Figure 1a),[1d] investigations of the optical properties of these types of positively charged boracyclic species have only recently gained attention.[4] Our laboratory synthesized a series of borafluorenium and borepinium ions and uncovered preliminary evidence for unusual thermochromic properties, suggesting that boron cations may have untapped optical properties important for the development of stimuli-responsive materials (Figure 1b).[4c] In a report by Jäkle, extended conjugation resulted in increased fluorescence in diborenium ions compared to their monomeric counterparts (Figure 1c).[4f] Gilroy and co-workers have shown borenium ion-based formazanate dyes to be optically tunable reactivity probes (Figure 1d).[4d,e]

Carbenes have been employed throughout boron chemistry to stabilize reactive species, and we demonstrated that an N-heterocyclic carbene (NHC) borafluorenium ion exhibits thermochromism in solution as a result of intermolecular boron−oxygen interactions.[4c] However, this compound (Figure 1b) was highly reactive and sensitive to protonation at low concentrations, even in rigorously dried solvent. Such challenges have limited the in-depth optical spectroscopic study of these molecules.[4c] While carbenes feature carbon(II) centers with a free σ-electron pair, carbones, a lesser-known class of carbon donor ligands, possess a carbon(0) center with the ability to donate *both* σ- and π-electron density to Lewis acidic fragments.[5] In this regard, it should be noted that Alcarazo,[6] Kuzu,[7] and Ye,[8] have isolated carbodiphosphorane-stabilized borenium ions (Figure 1e), and Ong utilized a carbodicarbene to stabilize a dicationic tricoordinate hydridoboron species (Figure 1f).[9]

One of the key types of optical materials being explored are tailor-made "smart" or stimuli-responsive materials that

Received: November 9, 2021
Published: January 4, 2022

https://doi.org/10.1021/jacs.1c11861
J. Am. Chem. Soc. 2022, 144, 590−598

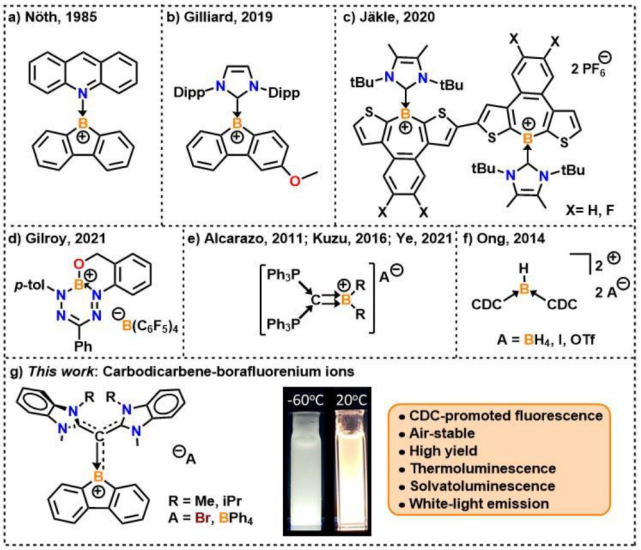

Figure 1. (a) Acridine-stabilized borafluorenium ion; (b) N-heterocyclic carbene (NHC)-stabilized borafluorenium ion (Dipp = 2,6-diisopropylphenyl); (c) NHC-diborepinium ion dimers; (d) formazanate borenium ion; (e) carbodiphosphorane-borenium ions [Alcarazo (2011), R = H, A = $HB(C_6F_5)_3$; Kuzu (2016), R = F, A = BF_4; Ye (2021), R = Br, Aryl, $O(CH_2)_4Br$, A = Br]; (f) carbodicarbene (CDC)-stabilized dicationic hydridoboron complex; (g) carbodicarbene-borafluorenium ions (this work).

respond to external stimuli without the need for additional reagents.[10] Such materials have potential applications in medical and food packaging sectors, where the temperature of a substance needs to be tracked "by eye" in the absence of expensive analytical equipment. We reasoned that it would be possible to rationally design temperature-responsive materials by exploiting the Lewis acidity of borenium ions. However, the typically reactive nature of this compound class would need to be overcome, and possible methods to achieve this goal are (1) to embed the cationic boron center in extended conjugated networks, decreasing the electrophilicity by dispersing the positive charge,[4a,f,11] or (2) to control the electrophilicity and reactivity using ligand-based strategies.[2,3i,4d] Due to the unique donor capabilities of carbones, carbodicarbene (CDC) was a potential candidate to mediate the chemistry. Indeed, we hypothesized that employing exceptionally strong donor ligands should result in borenium ions with enhanced stability and distinct optical properties resulting from ligand-to-boron cation π-conjugation. Herein, we report the synthesis, molecular structures, and absorption and emission behavior of carbodicarbene-stabilized borafluorenium ions (**2**, **3**, **6**) (Figure 1g). Notably, compounds **2**, **3**, and **6** represent the first examples of thermoluminescent borenium ions (i.e., the fluorescence of these compounds may be modulated based on temperature changes in solution). The emissive behavior is a result of synergistic effects between the π-donating carbodicarbene and the cationic boron heterocycle. To our knowledge, this is the first time CDC has been studied as a ligand for materials chemistry. We demonstrate that this single-molecule system exhibits temperature-controlled white-light emission as well as aggregation-induced emission (AIE). Moreover, these compounds are air-stable on the benchtop in the solid state for at least 1 week without any noticeable decomposition.

RESULTS AND DISCUSSION

A nucleophilic bromide displacement reaction in toluene involving CDC[12] and 9-bromo-9-borafluorene (**1**)[13] led to the CDC-stabilized borafluorenium ion (**2**), which was isolated in 93% yield as a bright yellow solid (Scheme 1). This was

Scheme 1. Synthesis of CDC-Stabilized Borafluorenium Ions

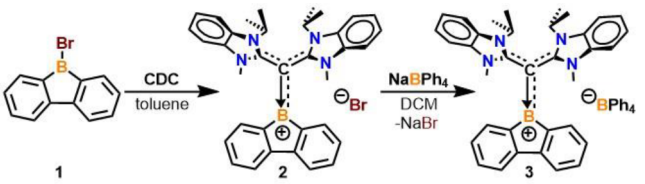

evident after characterization via $^{11}B\{^1H\}$ NMR, which displays a downfield chemical shift (48.4 ppm) in the range of tricoordinate borafluorenium ions.[1d,4c] The reactivity of CDC with 9-halo-9-borafluorene differs from weaker carbon donors such as carbenes, which form tetracoordinate borafluorenes[13,14] and require halide abstraction reactions for the synthesis of borenium ions.[4c] In order to assess the impact of anion sterics and possible weak coordination to the boron center, compound **2** was subjected to an anion exchange reaction with sodium tetraphenylborate ($NaBPh_4$) to give the borafluorenium ion **3**. Compound **3** was obtained as a bright yellow solid in 90% isolated yield and displayed $^{11}B\{^1H\}$ NMR signals at 48.3 (boron cation) and −6.6 ppm (BPh_4 anion). Remarkably, in the solid state, these cations are stable under aerobic conditions for at least 1 week.[15] In contrast, the vast majority of borenium ions and CDC complexes of other Lewis acids are air-sensitive.[2]

Single crystals suitable for X-ray diffraction were grown by slow diffusion of diethyl ether (Et_2O) into methylene chloride (DCM) at room temperature (for **2**) and by cooling a DCM/Et_2O mixture to −37 °C in the glovebox freezer (for **3**). In both instances, no contacts are observed between the cationic boron center and the counteranion, resulting in a trigonal planar geometry about the B1 atoms (Figure 2). The B^+ center in **2** being free of anion contacts is attributed to CDC's strong σ- and π-donor capability.[5d] The C1−B1 bond distance [1.485(4) Å (**2**); 1.495(3) Å (**3**)] is shorter than reported carbene-borafluorenium ions [1.567(5)−1.586(6) Å][4c] and more consistent with a carbon−boron double bond.[16] These values are similar to reported carbodiphosphorane-borenium ions [1.500(7)−1.514(5) Å].[6−8] The C1−C2 bond distances [1.454(4) Å (**2**); 1.436(3) Å (**3**)] are elongated with respect to the free CDC ligand [1.3455(16) Å], supporting increased donation of electron density from the ligand. Both crystal structures displayed a twisted CDC, with the two $N-CH_3$ groups oriented downward toward opposite sides of the borafluorene π-system. The angles between the NHC fragments were measured with planes drawn through all of the atoms in the five-membered NHC rings and demonstrated smaller interplanar angles in compound **2** [73.254(181)°] compared to compound **3** [80.256(91)°]. The nature of the C1−B1 bond in **2** was investigated theoretically using energy decomposition analysis with natural orbitals for chemical valence (EDA-NOCV). The stabilization in **2** and **3** arises principally from carbone to borenium σ-donation (68%), with partial π-donation (16%). NBO calculations identify both σ-

https://doi.org/10.1021/jacs.1c11861
J. Am. Chem. Soc. 2022, 144, 590−598

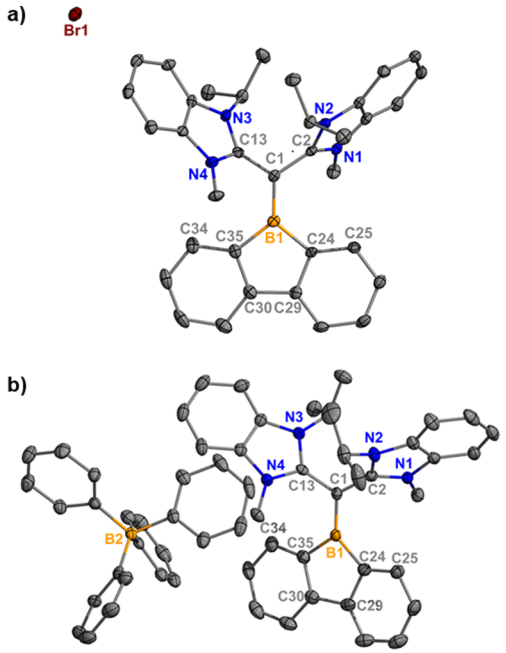

Figure 2. Molecular structures of **2** (a) and **3** (b) (thermal ellipsoids at 50% probability; H atoms and cocrystallized solvent (**3**, THF) omitted for clarity). Selected bond lengths [Å]: **2**: B1−C1 1.485(4), C1−C2 1.454(4), B1−C24 1.592(4), C2−N1 1.352(3); **3**: B1−C1 1.495(3), C1−C2 1.436(3), B1−C24 1.583(3), C2−N1 1.355(3).

and π-bonding orbitals between C1 and B1, both polarized toward C1. The natural population charge (NPA) on boron is +0.708, indicating the majority of the positive charge is localized on boron. From these analyses, the bond is best described by a coordinate covalent bond, represented by an arrow, with moderate π-electronic delocalization between the two fragments, represented by the dashed lines. A comprehensive analysis of the bonding parameters is provided in the Supporting Information.

The ^{1}H NMR spectra of compounds **2** and **3** showed two sets of CDC-borafluorenium ion peaks at room temperature in approximately a 2:1 ratio with some of the signals in the minor species appearing broadened (e.g., N−CH_3, N−CH(CH_3)$_2$, N−CH(CH_3)$_2$). The two species in solution were shown to be in direct chemical exchange, indicated by nuclear Overhauser effect spectroscopy (NOESY, Figure S9). We have attributed the second set of peaks to conformational changes as a result of rotation about the ^{carbone}C1−C2^{carbene} and ^{carbone}C1−C13^{carbene} bonds, as well as a weak intramolecular agostic interaction between the N−CH_3 protons and cationic boron center (Figure 3). Rotation about the carbone C−C bonds has been previously reported with a carbodicyclopropenylidene ligand.[17] Variable-temperature (VT) ^{1}H NMR data were obtained, in which the minor conformer signals N−CH_3, N−CH(CH_3)$_2$, C25−H, and C34−H split into two signals below 0 °C (Figures S4 and S15). A portion of the VT ^{1}H NMR spectrum of **2** with peak labels is shown alongside the proposed equilibrium process in Figure 3. High-temperature ^{1}H NMR studies indicate that all of the peaks coalesce by 120 °C, which supports an increased rotation of the ^{carbone}C−C^{carbene} bonds, and the presence of one species in solution (Figure S5).

The proposed weak, agostic interaction is supported by broadened N−CH_3 and N−CH(CH_3)$_2$ signals at room temperature in the minor species that split into two signals

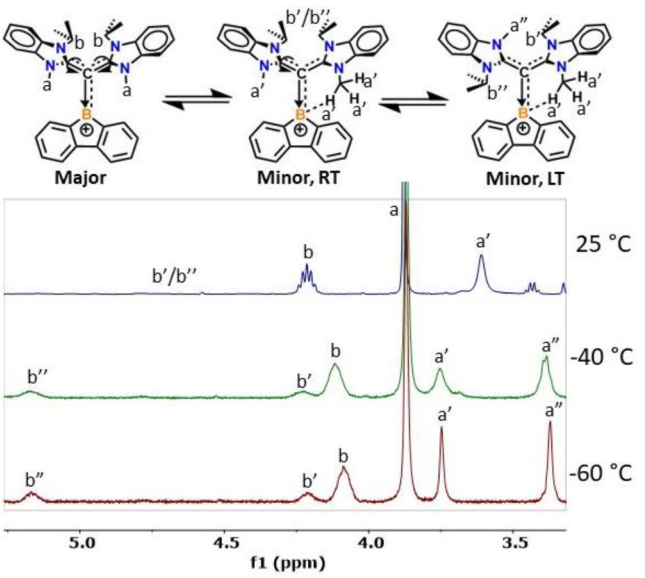

Figure 3. VT ^{1}H NMR of compound **2** at 3.3−5.3 ppm and proposed solution-state equilibrium at room temperature (RT) and low temperature (LT). See Figure S4 for the full spectrum.

at low temperature (Figure 3, minor, low temperature (LT)). The molecular structures of compounds **2** and **3** show the C−H bond and boron p_z orbital to be nearly coplanar in the solid state, and the closest H−B distances [2.657 Å (**2**); 2.688 Å (**3**)] are similar to a previously reported agostic interaction between a boron atom and a C−H bond on an ethane fragment [2.64 Å].[18] Theoretical analysis of the noncovalent interaction (NCI) surfaces between N−CH_3 protons and the borenium center reveals a weak covalent attraction typical of agostic interactions (Figure S50). Furthermore, NBO second-order perturbation analysis identifies two N−CH_3 $\sigma_{(C-H)} \rightarrow \pi^*_{(B-C)}$ donor−acceptor interactions with moderate stabilization energies ($E(2)$ = 12.6 kJ mol^{-1}).

To provide additional experimental support for this interaction, compound **2** was reacted with potassium bis(trimethylsilyl)amide (KHMDS) to afford compound **4** in 54% yield (Scheme 2). Upon interaction with the boron center, the

Scheme 2. Deprotonation and Cyclization of CDC-Stabilized Borafluorenium Ion 2

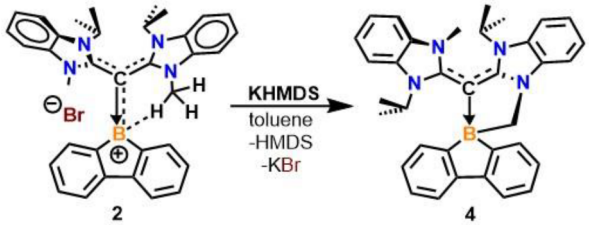

C−H bond on the N−CH$_3$ group is rendered more acidic, facilitating a deprotonation reaction and formation of a new five-membered ring. It should be noted that deprotonation does not occur with the addition of KHMDS to uncoordinated CDC, and this reaction is similar to what we observed in a previous study at a highly polarizing beryllium center.[5j,19] Crystals suitable for single-crystal X-ray diffraction were grown from the slow diffusion of hexane into a concentrated toluene solution of **4** at room temperature (Figure S46). The ^{11}B{^{1}H}

https://doi.org/10.1021/jacs.1c11861
J. Am. Chem. Soc. 2022, 144, 590−598

NMR spectrum shows a distinct upfield shift at −2.0 ppm, representative of a tetracoordinate boron center.

To further support our claim of conformational changes resulting in multiple proton environments, a symmetric CDC with N−CH_3 groups was synthesized (**5**).[5d] Upon coordination of **5** with compound **1** in toluene, compound **6** formed as a yellow precipitate in 91% yield (Scheme 3). Single crystals

Scheme 3. Synthesis of a Symmetric CDC-Borafluorenium Ion

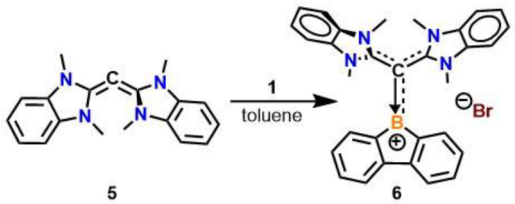

suitable for X-ray diffraction were grown from slow diffusion of Et_2O into DCM at room temperature (Figure S47). The $^{11}B\{^1H\}$ NMR spectrum of **6** showed a broad signal at 48.1 ppm, which is comparable to **2** and **3**. The ^1H NMR spectrum at room temperature showed one set of signals for the product, with a broadened signal for the N−CH_3 protons at 3.70 ppm. At −40 °C, the N−CH_3 protons split into two equivalent singlets indicating slowed $^{carbone}C-C^{carbene}$ rotation and interaction with the cationic boron, similar to compounds **2** and **3** (Figure S26). Therefore, the different conformers of the CDC ligand are indeed responsible for the two sets of signals observed in the ^1H NMR spectrum.

To study the photophysical properties of compounds **2**, **3**, and **6**, VT UV−vis and fluorescence spectroscopy, absolute quantum yield measurements, and fluorescence lifetime studies were performed. UV−vis data indicate that multiple excited states are accessible with three similar absorption events observed for the three cations around 265, 355, and 390 nm (Figure 4a). Time-dependent density functional theory (TD-DFT) calculations (CAM-B3LYP-D3(BJ)/def2-TZVP(SMD, DCM)) for **2** reveal the lowest energy transition ($S_0 \rightarrow S_1$) is an intramolecular charge transfer (CT) state (HOMO → LUMO) from the donor CDC moiety to the borafluorene acceptor (Table 1). The CT character of S_1 was confirmed by

Table 1. Calculated Vertical Excitation Energies of 2 at the CAM-B3LYP-D3(BJ)/def2-TZVP//B3LYP-D3(BJ)/def2-TZVP (SMD, DCM) Level of Theory

state	λ_{abs} (nm)[a]	f	excitation
S_1	396.8	0.555	HOMO → LUMO
S_2	388.1	0.007	HOMO−1 → LUMO
S_3	349.7	0.703	HOMO → LUMO+1

[a]Calculated vertical excitation energies corrected by −0.3 eV.

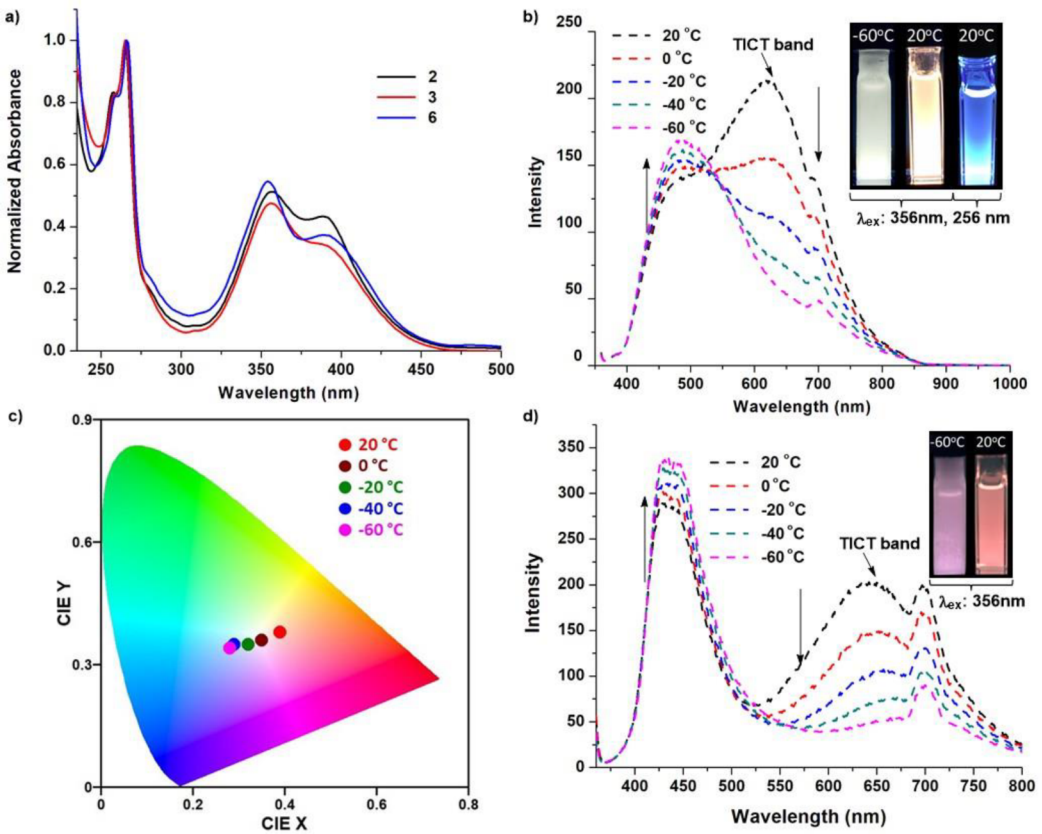

Figure 4. (a) Normalized UV−vis spectra for compounds **2**, **3**, and **6** in DCM. (b) VT fluorescence spectra for compound **2** in DCM (λ_{ex}: 350 nm [0.0125 mM]). Images: λ_{ex}: 356 nm (left, white and orange emission), 265 nm (right, blue emission). (c) CIE (1931) chromaticity diagram for compound **2** fluorescence in DCM at different temperatures [20 °C (0.39, 0.38), 0 °C (0.35, 0.36), −20 °C (0.32, 0.35), −40 °C (0.29, 0.35), −60 °C (0.28, 0.34)]. (d) VT fluorescence spectra for compound **6** in DCM (λ_{ex}: 350 nm [0.01 mM]). Images: λ_{ex}: 356 nm. Note: Spectral feature at 700 nm is a result of second-order Rayleigh scattering; no filter was used.

https://doi.org/10.1021/jacs.1c11861
J. Am. Chem. Soc. 2022, 144, 590−598

analysis of the natural transition orbitals and by plotting the differences in the electron densities for S_1 and S_0 (Figure 5).

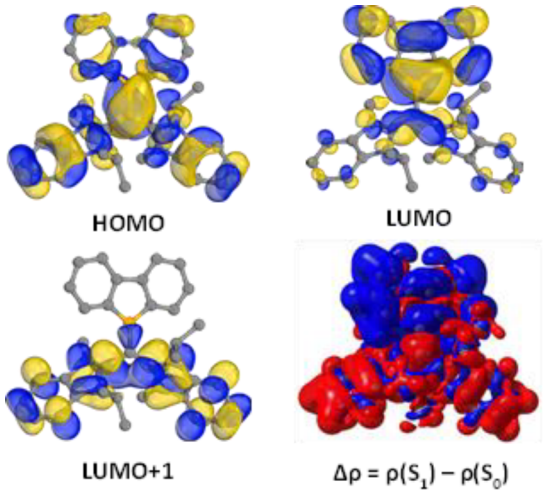

Figure 5. Frontier molecular orbitals of **2** calculated at the CAM-B3LYP-D3(BJ)/def2-TZVP//B3LYP-D3(BJ)/def2-TZVP (SMD, DCM) level of theory. Density difference plot between S_1 and S_0; electron density flows from red to blue (isosurface ±0.0001*e*). Hydrogen atoms are omitted for clarity.

The second excited state ($S_0 \rightarrow S_2$) is described by a weakly allowed transition (f = 0.007) centered on borafluorene. The third excited state ($S_0 \rightarrow S_3$) describes a $\pi \rightarrow \pi^*$ local (ligand-centered) excitation on CDC (HOMO → LUMO+1). The band observed for high-energy excitations (<280 nm) corresponds to local transitions centered on either the CDC or borafluorene ligands.

Excitation of compound **2** in DCM at 260 nm results in a bright blue fluorescence with a maximum peak at 450 nm (Figure S31). When excited at a longer wavelength (350 nm), the observed fluorescence is orange-yellow in color, and a strong peak at 620 nm is observed (Figure 4b). As the solution is cooled, the peak at 620 nm steadily decreases as the shoulder at 490 nm increases, resulting in a color change that is readily observable by the naked eye. The observation of dual fluorescence is commonly attributed to a twisted intramolecular charge transfer (TICT) process,[20] whereby two geometrically distinct singlet excited states are present upon excitation, each with unique emission profiles.[21] A principle of TICT systems is that the donating ligand is conjugated to the acceptor. Although examples of donor−acceptor TICT complexes can be found in the literature,[10a,21,22] to date none possess a coordinating carbene ligand due to the lack of CT excitations. However, the electronic properties of the CDC complex are fundamentally different from analogous NHC and CAAC complexes. The CDC ligand leads to conjugation with the borafluorene acceptor that arises from significant B═C character. Molecular orbital (MO) calculations for **2**, together with NHC and CAAC analogues (Figure S56), indicate that the HOMO of **2** (Figure 5) is associated with B═C π-interaction (ligand−acceptor conjugation); however this MO is unoccupied (LUMO) in the NHC and CAAC analogues. Moreover, CDC affords a significantly larger HOMO−LUMO gap than NHC or CAAC.

Theoretical studies of **2** were employed to investigate the origin of the dual-fluorescence process. The optimized ground-state geometry exhibits a dihedral angle between the borafluorene and CDC planes of 27.2°. Geometry optimizations on the S_1 potential energy surface (PES) located a minimum in which the borafluorene is near perpendicular to the CDC plane with a dihedral angle of 75.5°. Scans of the S_1 PES with respect to the dihedral angle reveals a rotational barrier at 50° (ΔE = +21 kJ mol^{-1}) and a local minimum corresponding to the twisted conformation (Figure S52). The twisted minimum on the S_1 PES is calculated to be lower in energy relative to the locally excited (LE) state by 50 kJ mol^{-1}. Calculated vertical emission energies ($S_1 \rightarrow S_0$) display the general trend of red shifting the emission wavelength with increasing dihedral angle (Figure S53). Theoretical state-specific absorption and emission energies for both the LE and TICT states are in excellent agreement with experiment. Figure 6 shows the potential energy diagram of **2**. Calculated emission

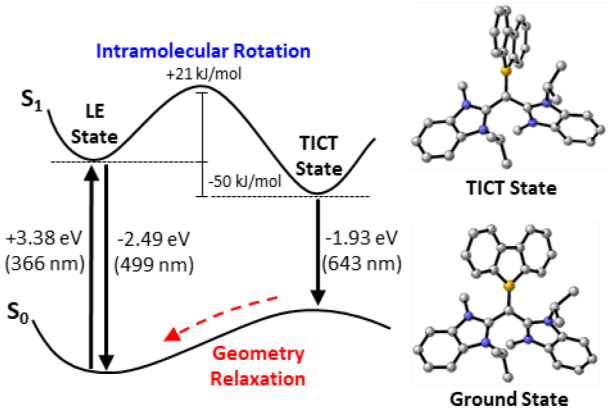

Figure 6. Potential energy diagram of **2**. State-specific absorbance/emission energies calculated at the CAM-B3LYP-D3(BJ)/def2-SVP//CAM-B3LYP-D3(BJ)/def2-TZVP (cLR, DCM). Hydrogen atoms are omitted for clarity.

at 499 nm is attributed to the LE state ($S_{1(LE)} \rightarrow S_0$); the borafluorene moiety then undergoes intramolecular rotation, whereby a second emission was calculated at 643 nm ($S_{1(TICT)} \rightarrow S_0$). At reduced temperatures, rotation about the C1−B1 bond is inhibited, resulting in a blue shift of the emission maxima corresponding to the locally excited state. The observed internal rotation is driven by total charge separation between the donor and acceptor fragments and the accompanying solvent relaxation.[22c] Excitations at high energy wavelengths (<280 nm) were calculated to be $\pi \rightarrow \pi^*$ transitions centered on borafluorene and CDC. Due to the lack of charge-separated higher energy singlet states, only the locally excited band ($S_{1(LE)} \rightarrow S_0$) is observed upon excitation at 260 nm.

The International Commission of Illumination (CIE) diagram[23] of **2** clearly depicts a color change occurring throughout the cooling process (Figure 4c). At 0 and −20 °C the CIE coordinates are (0.35, 0.36) and (0.32, 0.35), respectively, which are very close to the coordinates for pure white light (0.33, 0.33).[24] White-light emitters are sought after due to their importance in display technology and are often made through a method termed additive mixing, by which two complementary colors are combined to create white light.[24] A single-molecular system that achieves this feat is desirable because of its color stability, quantum efficiency, and a simpler device fabrication process.[24b]

https://doi.org/10.1021/jacs.1c11861
J. Am. Chem. Soc. 2022, 144, 590−598

Table 2. Quantum Yield Data and Fluorescence Lifetimes for Compounds 2, 3, and 6

compound	Φ_F[single crystals][a]	Φ_F[dropcast][b]	Φ_F[solution][c]	Φ_F[solution][d]	τ_s1/ns[e]	τ_s2/ns[e]
2	0.291	0.245	0.060	0.041	0.2 (43%)	1.1 (57%)
3	0.177	0.211	0.074	0.032	0.4 (31%)	1.6 (69%)
6	0.199	0.151	0.086	0.061	0.3 (85%)	2.6 (15%)

[a]QY of single crystals. [b]QY of drop-cast samples, single crystals dissolved in DCM (10 mg/1 mL). [c]QY of sample in DCM, λ_{ex} = 265 nm. [d]QY of sample in DCM, λ_{ex} = 350 nm. [e]Fluorescence lifetimes measured in dichloromethane at 920 nm at room temperature; values in parentheses indicate the relative amplitude weightings of the pre-exponential factors.

When compound **2** is dissolved in chlorobenzene, differences in the UV−vis spectrum are observed with a λ_{max} at 390 nm and a small shoulder at 350 nm (Figure S32). Excitation of this sample at 350 nm results in a bright blue fluorescence at 427 nm and no observable TICT feature (Figure S33). This is in stark contrast to the orange-yellow fluorescence color in DCM and indicates solvatoluminescence, although further studies were limited by the insolubility of the compound. The difference in fluorescence can likely be attributed to the difference in polarity for DCM (ε = 9.14) and chlorobenzene (ε = 5.69),[25] whereas DCM is able to stabilize a large dipole moment in the TICT state of **2**.

Fluorescence studies of compound **3** were carried out in DCM, and excitation at 350 nm exhibited thermoluminescence. The emission of compound **3** closely resembled compound **2**, with a bright yellow-orange fluorescence observed at room temperature and a peak at 628 nm that decreased along with cooling and a peak at 444 nm that increased at low temperatures (Figure S38A). A plot of the CIE chromaticity diagram shows a similar trend relative to compound **2**, although at lower temperatures, **3** does not show emission passing through the white-light region (Figure S38B). A comparison between two different CDCs offered a visible difference with a pink fluorescence observed at room temperature for compound **6** (λ_{ex} = 350 nm). Fluorescence spectroscopy showed prominent peaks at 434 and 644 nm (Figure 4d). The peak at 644 nm decreases as the solution is cooled, whereas the peak at 434 nm increases at lower temperatures (see the Supporting Information for theoretical results). The peak associated with TICT is red-shifted in all three species, which is consistent with a longer fluorescence lifetime. To determine the contribution of the fluorescence of both LE and TICT states, time-resolved fluorescence measurements were performed. The decay processes of **2**, **3**, and **6** were fit using a biexponential model with photoluminescence data summarized in Table 2. Expectedly, the lifetime of the LE state (τ1) is shorter than the TICT state (τ2), and the radiative and nonradiative decay rate constants can be found in Table S1.

During our collection of the quantum yields (QYs) of these compounds, we observed large differences between the data when collected in solution versus the solid state. Therefore, we performed quantum yield studies on the single crystals, drop-cast samples, and solutions at two different wavelengths (Figure 7). The data corresponding to the images in Figure 7 are summarized in Table 2. A comparison of the QYs between phases for each compound shows that compounds **2** and **6** have the highest QYs as single crystals, whereas compound **3** has its highest quantum yield when drop-casted. We observe a significant decrease in fluorescence efficiency in solution, with the lowest values for all three compounds when λ_{ex} = 350 nm. This is consistent with the observed TICT process, as charge transfer species typically have lower QYs.[22e,26] The observed

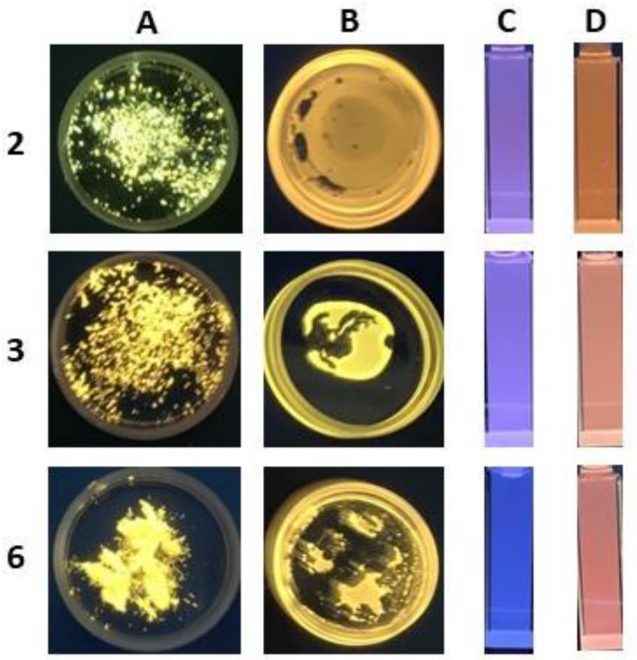

Figure 7. Images of the samples used for QY measurements of compounds **2**, **3** and **6**: (A) Single crystals, λ_{ex} = 365 nm. (B) Drop-casted in DCM at room temperature, λ_{ex} = 365 nm. (C) DCM solutions, λ_{ex} = 265 nm. (D) DCM solutions, λ_{ex} = 356 nm.

AIE can be attributed to the restricted TICT process in the solid state.

We have synthesized and fully characterized the first examples of thermoluminescent borenium ions. The temperature-responsive properties result from the synergistic combination of carbodicarbene and a B^+-doped heterocycle, which elicits a TICT process. Significantly, these complexes are air-stable in the solid state, which bodes well for future applications. The first utilization of carbones as a ligand in materials-relevant chemistry highlights key electronic differences between carbones and carbenes. Indeed, it is noteworthy that these materials are distinctly different, in both bonding and optical properties, from NHC-stabilized borafluorenium ions, which were air-sensitive, nonemissive, and decomposed at low concentrations.[4c] The solution-state properties of CDC-borafluorenium ions were thoroughly studied via NMR and indicate different conformational states of the CDC ligand and evidence for an intramolecular agostic interaction. The optical properties of cations **2**, **3**, and **6** were characterized by UV−vis and fluorescence spectroscopy, and their solid-state QYs were relatively high for a structurally unique TICT-based donor−acceptor compound. The results from these studies showed thermoluminescence, TICT-based AIE, and temperature-responsive white-light emission. These properties are typically observed in highly conjugated complex systems or polymers;

https://doi.org/10.1021/jacs.1c11861
J. Am. Chem. Soc. 2022, 144, 590−598

thus, a single-molecule system exhibiting this behavior is desirable. Collectively, the chemistry presented is counter-intuitive and represents a departure from commonly held perceptions of charged tricoordinate boron compounds: that they are laboratory curiosities that are highly reactive. This CDC-based approach, which leads to π-conjugation between the ligand and the B^+-doped heterocycle, may serve as a general strategy for the development of stable temperature-responsive materials featuring cationic boron.

■ ASSOCIATED CONTENT

Supporting Information

The Supporting Information is available free of charge at https://pubs.acs.org/doi/10.1021/jacs.1c11861.

Experimental details, NMR spectra, photophysical data, single-crystal X-ray diffraction data, and computational details (PDF)

Accession Codes

CCDC 2118230−2118233 contain the supplementary crystallographic data for this paper. These data can be obtained free of charge via www.ccdc.cam.ac.uk/data_request/cif, or by emailing data_request@ccdc.cam.ac.uk, or by contacting The Cambridge Crystallographic Data Centre, 12 Union Road, Cambridge CB2 1EZ, UK; fax: +44 1223 336033.

■ AUTHOR INFORMATION

Corresponding Authors

David J. D. Wilson − *Department of Chemistry and Physics, La Trobe Institute for Molecular Science, La Trobe University, Melbourne 3086 Victoria, Australia;* orcid.org/0000-0002-0007-4486; Email: david.wilson@latrobe.edu.au

Robert J. Gilliard, Jr. − *Department of Chemistry, University of Virginia, Charlottesville, Virginia 22904, United States;* orcid.org/0000-0002-8830-1064; Email: rjg8s@virginia.edu

Authors

Kimberly K. Hollister − *Department of Chemistry, University of Virginia, Charlottesville, Virginia 22904, United States;* orcid.org/0000-0001-9024-4436

Andrew Molino − *Department of Chemistry and Physics, La Trobe Institute for Molecular Science, La Trobe University, Melbourne 3086 Victoria, Australia;* orcid.org/0000-0002-0954-9054

Grace Breiner − *Department of Chemistry, University of Virginia, Charlottesville, Virginia 22904, United States*

Jacob E. Walley − *Department of Chemistry, University of Virginia, Charlottesville, Virginia 22904, United States;* orcid.org/0000-0003-1495-6823

Kelsie E. Wentz − *Department of Chemistry, University of Virginia, Charlottesville, Virginia 22904, United States;* orcid.org/0000-0002-0464-8010

Ashley M. Conley − *Department of Chemical Engineering, University of Virginia, Charlottesville, Virginia 22904, United States*

Diane A. Dickie − *Department of Chemistry, University of Virginia, Charlottesville, Virginia 22904, United States;* orcid.org/0000-0003-0939-3309

Complete contact information is available at: https://pubs.acs.org/10.1021/jacs.1c11861

Author Contributions

The manuscript was written through contributions of all authors. All authors have given approval to the final version of the manuscript.

Notes

The authors declare no competing financial interest.

■ ACKNOWLEDGMENTS

We are grateful to the University of Virginia (UVA) and the National Science Foundation Chemical Synthesis (CHE 2046544), and Major Research Instrumentation (CHE 2018870) programs for support of this work. R.J.G. acknowledges additional laboratory support through a Sloan Research Fellowship provided by the Alfred P. Sloan Foundation and a Beckman Young Investigator award from the Arnold & Mabel Beckman Foundation. We acknowledge Dr. Jeffery Ellena, biomolecular magnetic resonance facilities manager at UVA, for helpful discussions regarding NMR assignments. The Keck Center for Cellular Imaging at UVA is also acknowledged for the usage of a Zeiss 780 microscopy system (PI:AP; NIH-OD016446) for fluorescence lifetime measurements. Generous allocation of computing resources from the National Computational Infrastructure (NCI), Intersect, and La Trobe University is acknowledged.

■ REFERENCES

(1) (a) Koelle, P.; Noeth, H. The chemistry of borinium and borenium ions. *Chem. Rev.* **1985**, *85*, 399−418. (b) Narula, C. K.; Nöth, H. Preparation and characterization of salts containing cations of tricoordinate boron. *Inorg. Chem.* **1984**, *23*, 4147−4152. (c) Narula, C. K.; Nöth, H. A novel trico-ordinated boronium salt: 1,3-dimethyl-2-phenanthridin-5-yl-1,3,2-diazaborolidinium trifluoromethansesulphonate. *J. Chem. Soc., Chem. Comm.* **1984**, *15*, 1023−1024. (d) Narula, C. K.; Noeth, H. Contribution to the chemistry of boron. 150. Competition between adduct and cation formation in reactions between diorganylborane derivatives and pyridine or lutidines. *Inorg. Chem.* **1985**, *24*, 2532−2539.

(2) For reviews on this topic: (a) Piers, W. E.; Bourke, S. C.; Conroy, K. D. Borinium, Borenium, and Boronium Ions: Synthesis, Reactivity, and Applications. *Angew. Chem., Int. Ed.* **2005**, *44*, 5016−5036. (b) Franz, D.; Inoue, S. Cationic Complexes of Boron and Aluminum: An Early 21st Century Viewpoint. *Chem.—Eur. J.* **2018**, *25*, 2898−2926.

(3) For reviews on this topic: (a) Eisenberger, P.; Crudden, C. M. Borocation catalysis. *Dalton Trans.* **2017**, *46*, 4874−4887. (b) De Vries, T. S.; Prokofjevs, A.; Vedejs, E. Cationic Tricoordinate Boron Intermediates: Borenium Chemistry from the Organic Perspective. *Chem. Rev.* **2012**, *112*, 4246−4282. (c) Ingleson, M. J. Fundamental and Applied Properties of Borocations. In *Synthesis and Application of Organoboron Compounds*, Fernández, E.; Whiting, A., Eds.; Springer International Publishing: Cham, 2015, DOI: 10.1007/978-3-319-13054-5_2pp 39-71. (d) Rao, B.; Kinjo, R. Boron-Based Catalysts for C−C Bond-Formation Reactions. *Chem.—Asian J.* **2018**, *13*, 1279−1292. For selected publications on this topic: (e) Farrell, J. M.; Hatnean, J. A.; Stephan, D. W. Activation of Hydrogen and Hydrogenation Catalysis by a Borenium Cation. *J. Am. Chem. Soc.* **2012**, *134*, 15728−15731. (f) Mercea, D. M.; Howlett, M. G.; Piascik, A. D.; Scott, D. J.; Steven, A.; Ashley, A. E.; Fuchter, M. J. Enantioselective reduction of N-alkyl ketimines with frustrated Lewis pair catalysis using chiral borenium ions. *Chem. Commun.* **2019**, *55*, 7077−7080. (g) Lam, J.; Günther, B. A. R.; Farrell, J. M.; Eisenberger, P.; Bestvater, B. P.; Newman, P. D.; Melen, R. L.; Crudden, C. M.; Stephan, D. W. Chiral carbene−borane adducts: precursors for borenium catalysts for asymmetric FLP hydrogenations. *Dalton Trans.* **2016**, *45*, 15303−15316. (h) Farrell, J. M.; Posaratnanathan, R. T.; Stephan, D. W. A family of N-heterocyclic carbene-stabilized

borenium ions for metal-free imine hydrogenation catalysis. *Chem. Sci.* **2015**, *6*, 2010−2015. (i) Farrell, J. M.; Stephan, D. W. Planar N-Heterocyclic Carbene Diarylborenium Ions: Synthesis by Cationic Borylation and Reactivity with Lewis Bases. *Angew. Chem., Int. Ed.* **2015**, *54*, 5214−5217. (j) Cao, L. L.; Stephan, D. W. Homolytic Cleavage Reactions of a Neutral Doubly Base Stabilized Diborane(4). *Organometallics* **2017**, *36*, 3163−3170.

(4) (a) Tsurumaki, E.; Hayashi, S.-y.; Tham, F. S.; Reed, C. A.; Osuka, A. Planar Subporphyrin Borenium Cations. *J. Am. Chem. Soc.* **2011**, *133*, 11956−11959. (b) Bonnier, C.; Piers, W. E.; Parvez, M.; Sorensen, T. S. Borenium cations derived from BODIPY dyes. *Chem. Commun.* **2008**, *38*, 4593−4595. (c) Yang, W.; Krantz, K. E.; Freeman, L. A.; Dickie, D. A.; Molino, A.; Kaur, A.; Wilson, D. J. D.; Gilliard, R. J., Jr. Stable Borepinium and Borafluorenium Heterocycles: A Reversible Thermochromic "Switch" Based on Boron-Oxygen Interactions. *Chem.—Eur. J.* **2019**, *25*, 12512−12516. (d) Maar, R. R.; Katzman, B. D.; Boyle, P. D.; Staroverov, V. N.; Gilroy, J. B. Cationic Boron Formazanate Dyes**. *Angew. Chem., Int. Ed.* **2021**, *60*, 5152−5156. (e) Katzman, B. D.; Maar, R. R.; Cappello, D.; Sattler, M. O.; Boyle, P. D.; Staroverov, V. N.; Gilroy, J. B. A strongly Lewis-acidic and fluorescent borenium cation supported by a tridentate formazanate ligand. *Chem. Commun.* **2021**, *57*, 9530−9533. (f) Adachi, Y.; Arai, F.; Jäkle, F. Extended conjugated borenium dimers via late stage functionalization of air-stable borepinium ions. *Chem. Commun.* **2020**, *56*, 5119−5122. For a recent study on luminescent neutral borafluorenes see selected reference and references therein: (g) Rauch, F.; Fuchs, S.; Friedrich, A.; Sieh, D.; Krummenacher, I.; Braunschweig, H.; Finze, M.; Marder, T. B. Highly Stable, Readily Reducible, Fluorescent, Trifluoromethylated 9-Borafluorenes. *Chem.—Eur. J.* **2020**, *26*, 12794−12808.

(5) (a) Hermann, M.; Frenking, G. Carbones as Ligands in Novel Main-Group Compounds E[C(NHC)2]2 (E = Be, B+, C2+, N3+, Mg, Al+, Si2+, P3+): A Theoretical Study. *Chem.—Eur. J.* **2017**, *23*, 3347−3356. (b) Tonner, R.; Frenking, G. C(NHC)2: Divalent Carbon(0) Compounds with N-Heterocyclic Carbene Ligands—Theoretical Evidence for a Class of Molecules with Promising Chemical Properties. *Angew. Chem., Int. Ed.* **2007**, *46*, 8695−8698. (c) Munz, D. Pushing Electrons—Which Carbene Ligand for Which Application? *Organometallics* **2018**, *37*, 275−289. (d) Dyker, C. A.; Lavallo, V.; Donnadieu, B.; Bertrand, G. Synthesis of an Extremely Bent Acyclic Allene (A "Carbodicarbene"): A Strong Donor Ligand. *Angew. Chem., Int. Ed.* **2008**, *47*, 3206−3209. (e) Klein, S.; Tonner, R.; Frenking, G. Carbodicarbenes and Related Divalent Carbon(0) Compounds. *Chem.—Eur. J.* **2010**, *16*, 10160−10170. (f) Liu, S.-k.; Shih, W.-C.; Chen, W.-C.; Ong, T.-G. Carbodicarbenes and their Captodative Behavior in Catalysis. *ChemCatChem.* **2018**, *10*, 1480−1480. (g) Fürstner, A.; Alcarazo, M.; Goddard, R.; Lehmann, C. W. Coordination Chemistry of Ene-1,1-diamines and a Prototype "Carbodicarbene. *Angew. Chem., Int. Ed.* **2008**, *47*, 3210−3214. (h) Walley, J. E.; Warring, L. S.; Wang, G.; Dickie, D. A.; Pan, S.; Frenking, G.; Gilliard, R. J., Jr. Carbodicarbene Bismaalkene Cations: Unravelling the Complexities of Carbene versus Carbone in Heavy Pnictogen Chemistry. *Angew. Chem., Int. Ed.* **2021**, *60*, 6682−6690. (i) Walley, J. E.; Dickie, D. A.; Gilliard, R. J. Crystallographic study of a heteroleptic chloroberyllium borohydride carbodicarbene complex. *Z. Naturforsch. B* **2020**, *75*, 497−501. (j) Walley, J. E.; Breiner, G.; Wang, G.; Dickie, D. A.; Molino, A.; Dutton, J. L.; Wilson, D. J. D.; Gilliard, J. R. J. s-Block carbodicarbene chemistry: C(sp3)−H activation and cyclization mediated by a beryllium center. *Chem. Commun.* **2019**, *55*, 1967−1970.

(6) Inés, B.; Patil, M.; Carreras, J.; Goddard, R.; Thiel, W.; Alcarazo, M. Synthesis, Structure, and Reactivity of a Dihydrido Borenium Cation. *Angew. Chem., Int. Ed.* **2011**, *50*, 8400−8403.

(7) Münzer, J. E.; Oña-Burgos, P.; Arrabal-Campos, F. M.; Neumüller, B.; Tonner, R.; Fernández, I.; Kuzu, I. Difluoroborenium Cation Stabilized by Hexaphenyl-Carbodiphosphorane: A Concise Study on the Molecular and Electronic Structure of [(Ph3P)2C→BF2][BF4]. *Eur. J. Inorg. Chem.* **2016**, *24*, 3852−3858.

(8) Xiang, L.; Wang, J.; Su, W.; Lin, Z.; Ye, Q. Facile access to halogenated cationic B = C-centered organoborons isoelectronic with alkenyl halides. *Dalton Trans.* **2021**, *50*, 17491−17494.

(9) Chen, W.-C.; Lee, C.-Y.; Lin, B.-C.; Hsu, Y.-C.; Shen, J.-S.; Hsu, C.-P.; Yap, G. P. A.; Ong, T.-G. The Elusive Three-Coordinate Dicationic Hydrido Boron Complex. *J. Am. Chem. Soc.* **2014**, *136*, 914−917.

(10) For selected reviews on this topic: (a) Mellerup, S. K.; Wang, S. Boron-based stimuli responsive materials. *Chem. Soc. Rev.* **2019**, *48*, 3537−3549. (b) Mukherjee, S.; Thilagar, P. Stimuli and shape responsive 'boron-containing' luminescent organic materials. *J. Mater. Chem.* **2016**, *4*, 2647−2662.

(11) (a) Shimoyama, D.; Baser-Kirazli, N.; Lalancette, R. A.; Jäkle, F. Electrochromic Polycationic Organoboronium Macrocycles with Multiple Redox States. *Angew. Chem., Int. Ed.* **2021**, *60*, 17942−17946. (b) Gotoh, H.; Nakatsuka, S.; Tanaka, H.; Yasuda, N.; Haketa, Y.; Maeda, H.; Hatakeyama, T. Syntheses and Physical Properties of Cationic BN-Embedded Polycyclic Aromatic Hydrocarbons. *Angew. Chem., Int. Ed.* **2021**, *60*, 12835−12840.

(12) Chen, W.-C.; Shen, J.-S.; Jurca, T.; Peng, C.-J.; Lin, Y.-H.; Wang, Y.-P.; Shih, W.-C.; Yap, G. P. A.; Ong, T.-G. Expanding the Ligand Framework Diversity of Carbodicarbenes and Direct Detection of Boron Activation in the Methylation of Amines with CO2. *Angew. Chem., Int. Ed.* **2015**, *54*, 15207−15212.

(13) Berger, C. J.; He, G.; Merten, C.; McDonald, R.; Ferguson, M. J.; Rivard, E. Synthesis and Luminescent Properties of Lewis Base-Appended Borafluorenes. *Inorg. Chem.* **2014**, *53*, 1475−1486.

(14) (a) Su, X.; Bartholome, T. A.; Tidwell, J. R.; Pujol, A.; Yruegas, S.; Martinez, J. J.; Martin, C. D. 9-Borafluorenes: Synthesis, Properties, and Reactivity. *Chem. Rev.* **2021**, *121*, 4147−4192. (b) Wentz, K. E.; Molino, A.; Weisflog, S. L.; Kaur, A.; Dickie, D. A.; Wilson, D. J. D.; Gilliard, R. J., Jr. Stabilization of the Elusive 9-Carbene-9-Borafluorene Monoanion. *Angew. Chem., Int. Ed.* **2021**, *60*, 13065−13072.

(15) A systematic stability study of compounds **2** and **3** in which the ^{1}H NMR spectra of air-free samples were recorded as a baseline. Separate solid samples were then subjected to open air for one week and dissolved in the same NMR solvent, and then the ^{1}H NMR spectra were recorded. A visual assessment of the samples that were subjected to air and used for NMR analysis and the ^{1}H NMR spectra of the samples showed no evidence of decomposition. As the spectra were the same before and after air exposure, we concluded that the compounds were indeed stable. The language of "at least one week" was used because we did not test them beyond that point.

(16) (a) Groom, C. R.; Bruno, I. J.; Lightfoot, M. P.; Ward, S. C. The Cambridge Structural Database. *Acta Cryst. B* **2016**, *72*, 171−179. (b) Pranckevicius, C.; Herok, C.; Fantuzzi, F.; Engels, B.; Braunschweig, H. Bond-Strengthening Backdonation in Aminoborylene-Stabilized Aminoborylenes: At the Intersection of Borylenes and Diborenes. *Angew. Chem., Int. Ed.* **2019**, *58*, 12893−12897. (c) Wang, B.; Li, Y.; Ganguly, R.; Hirao, H.; Kinjo, R., Ambiphilic boron in 1,4,2,5-diazadiborinine *Nat. Commun.* **2016**, *7*, 11871. (d) Brückner, T.; Arrowsmith, M.; Heß, M.; Hammond, K.; Müller, M.; Braunschweig, H. Synthesis of fused B,N-heterocycles by alkyne cleavage, NHC ring-expansion and C−H activation at a diboryne. *Chem. Commun.* **2019**, *55*, 6700−6703.

(17) Pranckevicius, C.; Liu, L. L.; Bertrand, G.; Stephan, D. W. Synthesis of a Carbodicyclopropenylidene: A Carbodicarbene based Solely on Carbon. *Angew. Chem., Int. Ed.* **2016**, *55*, 5536−5540.

(18) Bluhm, M.; Maderna, A.; Pritzkow, H.; Bethke, S.; Gleiter, R.; Siebert, W. Synthesis of Tetraborylethenes and 1,1,1′,1′-Tetra- and Hexaborylethanes; Electronic Interactions in Tetraborylethenes and 1,1,1′,1′-Tetraborylethanes, and HF-SCF Calculations. *Eur. J. Inorg. Chem.* **1999**, *1999*, 1693−1700.

(19) Walley, J. E.; Obi, A. D.; Breiner, G.; Wang, G.; Dickie, D. A.; Molino, A.; Dutton, J. L.; Wilson, D. J. D.; Gilliard, R. J. Cyclic(alkyl)(amino) Carbene-Promoted Ring Expansion of a Carbodicarbene Beryllacycle. *Inorg. Chem.* **2019**, *58*, 11118−11126.

https://doi.org/10.1021/jacs.1c11861
J. Am. Chem. Soc. 2022, 144, 590−598

(20) Sasabe, H.; Kido, J. Multifunctional Materials in High-Performance OLEDs: Challenges for Solid-State Lighting. *Chem. Mater.* **2011**, *23*, 621−630.
(21) Lou, A. J. T.; Marks, T. J. A Twist on Nonlinear Optics: Understanding the Unique Response of π-Twisted Chromophores. *Acc. Chem. Res.* **2019**, *52*, 1428−1438.
(22) (a) Grabowski, Z. R.; Rotkiewicz, K.; Rettig, W. Structural Changes Accompanying Intramolecular Electron Transfer: Focus on Twisted Intramolecular Charge-Transfer States and Structures. *Chem. Rev.* **2003**, *103*, 3899−4032. (b) Lapouyade, R.; Czeschka, K.; Majenz, W.; Rettig, W.; Gilabert, E.; Rulliere, C. Photophysics of donor-acceptor substituted stilbenes. A time-resolved fluorescence study using selectively bridged dimethylamino cyano model compounds. *J. Phys. Chem.* **1992**, *96*, 9643−9650. (c) Rettig, W. Charge Separation in Excited States of Decoupled Systems—TICT Compounds and Implications Regarding the Development of New Laser Dyes and the Primary Process of Vision and Photosynthesis. *Angew. Chem., Int. Ed.* **1986**, *25*, 971−988. (d) Sudhakar, P.; Mukherjee, S.; Thilagar, P. Revisiting Borylanilines: Unique Solid-State Structures and Insight into Photophysical Properties. *Organometallics* **2013**, *32*, 3129−3133. (e) Taniguchi, T.; Wang, J.; Irle, S.; Yamaguchi, S. TICT fluorescence of N-borylated 2,5-diarylpyrroles: a gear like dual motion in the excited state. *Dalton Trans.* **2013**, *42*, 620−624. (f) Wang, J.; Wang, Y.; Taniguchi, T.; Yamaguchi, S.; Irle, S. Substituent Effects on Twisted Internal Charge Transfer Excited States of N-Borylated Carbazoles and (Diphenylamino)boranes. *J. Phys. Chem. A* **2012**, *116*, 1151−1158. (g) Zhang, Z.; Edkins, R. M.; Nitsch, J.; Fucke, K.; Steffen, A.; Longobardi, L. E.; Stephan, D. W.; Lambert, C.; Marder, T. B. Optical and electronic properties of air-stable organoboron compounds with strongly electron-accepting bis(fluoromesityl)boryl groups. *Chem. Sci.* **2015**, *6*, 308−321.
(23) Smith, T.; Guild, J. The C.I.E. colorimetric standards and their use. *Trans. Opt. Soc.* **1932**, *33*, 73−134.
(24) (a) Mukherjee, S.; Thilagar, P. Organic white-light emitting materials. *Dyes Pigm.* **2014**, *110*, 2−27. (b) Kundu, S.; Sk, B.; Pallavi, P.; Giri, A.; Patra, A. Molecular Engineering Approaches Towards All-Organic White Light Emitting Materials. *Chem.—Eur. J.* **2020**, *26*, 5557−5582.
(25) James, G. S. In *Lange's Handbook of Chemistry*, 17th ed.; McGraw-Hill Education: New York, 2017; Chapter 2.10.
(26) Wang, C.; Chi, W.; Qiao, Q.; Tan, D.; Xu, Z.; Liu, X. Twisted intramolecular charge transfer (TICT) and twists beyond TICT: from mechanisms to rational designs of bright and sensitive fluorophores. *Chem. Soc. Rev.* **2021**, *50*, 12656−12678.

https://doi.org/10.1021/jacs.1c11861
J. Am. Chem. Soc. 2022, 144, 590−598